

Quantum quenches in the Dicke model: Thermalization and failure of the generalized Gibbs ensemble

Xiao-Qiang Su(苏晓强)† and You-Quan Zhao(赵有权)
Citation: Chin. Phys. B, 2020, 29 (**12**): 120506. DOI: 10.1088/1674-1056/abc679
Journal homepage: http://cpb.iphy.ac.cn; http://iopscience.iop.org/cpb

What follows is a list of articles you may be interested in

Quantum quenches in the Dicke model: Thermalization and failure of the generalized Gibbs ensemble

Xiao-Qiang Su(苏晓强)† and You-Quan Zhao(赵有权)
Chin. Phys. B, 2020, 29 (**12**): 120506. DOI: 10.1088/1674-1056/abc679

A polaron theory of quantum thermal transistor in nonequilibrium three-level systems

Chen Wang(王晨), Da-Zhi Xu(徐大智)
Chin. Phys. B, 2020, 29 (**8**): 080504. DOI: 10.1088/1674-1056/ab973b

Symmetry properties of fluctuations in an actively driven rotor

He Li(李赫), Xiang Yang(杨翔), Hepeng Zhang(张何朋)
Chin. Phys. B, 2020, 29 (**6**): 060502. DOI: 10.1088/1674-1056/ab862b

Energy cooperation in quantum thermoelectric systems withmultiple electric currents

Yefeng Liu(刘叶锋), Jincheng Lu(陆金成), Rongqian Wang(王荣倩), Chen Wang(王晨), Jian-Hua Jiang(蒋建华)
Chin. Phys. B, 2020, 29 (**4**): 040504. DOI: 10.1088/1674-1056/ab7da5

Identifying the closeness of eigenstates in quantum many-body systems

Hai-bin Li(李海彬), Yang Yang(杨扬), Pei Wang(王沛), Xiao-guang Wang(王晓光)
Chin. Phys. B, 2017, 26 (**8**): 080502. DOI: 10.1088/1674-1056/26/8/080502

Quantum quenches in the Dicke model: Thermalization and failure of the generalized Gibbs ensemble*

Xiao-Qiang Su(苏晓强)† and You-Quan Zhao(赵有权)

College of Physics and Information Engineering, ShanXi Normal University, Linfen 041004, *China*

(Received 22 September 2020; revised manuscript received 18 October 2020; accepted manuscript online 31 October 2020)

Quantum quenches in the Dicke model were studied both in the thermodynamic limit and the finite systems. For the integrable situation in the thermodynamic limit, the generalized Gibbs ensemble can effectively describe the energy-level occupations for the quench within the normal phase, but it fails for the quench to the superradiant phase. For the finite systems which are considered non-integrable, the post quench systems were studied by comparing with the thermal ensembles. The canonical ensembles are directly available for the quench within the normal phase. With the increasing of the target coupling strength over the equilibrium phase transition critical point, sudden changes take place for the effective temperature and the distance to the thermal ensembles. The thermalization was also studied by comparing with the results of the microcanonical ensembles.

Keywords: quantum quench, generalized Gibbs ensemble, thermalization, Dicke model

PACS: 05.70.Ln, 02.30.Ik, 64.70.qd **DOI:** 10.1088/1674-1056/abc679

1. Introduction

Thermalization of the classical systems has been widely studied and successfully described by the statistical mechanics. In classical physics, it is known that the chaotic dynamics lead to ergodicity in the phase space, hence the time averages of the observables accord with the statistical ensembles. Thus we can describe the equilibrium systems by using a few parameters without the details of the microscopic dynamics. Recently, the reconstruction of the statistical mechanics based on the microscopic quantum theory becomes a hot topic. Whether a quantum system with unitary evolution eventually thermalizes? Which kinds of quantum systems out of equilibrium equilibrate and tend to a statistical ensemble. Rapid developments of the ultracold atoms experiments[1,2] have provided a platform to study the dynamics of the isolated quantum systems, promoting the researches on the nonequilibrium phenomena and quantum statistical mechanics.

The quantum quench,[3–7] which is achieved by suddenly changing the parameters of the quantum systems, is a natural method to study the quantum non-equilibrium dynamics. The system is prepared in an initial state ρ_0, which is mostly the ground state of the initial Hamiltonian H_0. Then the model parameters are quickly changed and the quantum system undergoes an unitary time evolution with the new Hamiltonian H. Thus the expectation values of an observable $\hat{A}$ can be obtained as

$$\langle \hat{A}(t) \rangle = \mathrm{tr}(\mathrm{e}^{-\mathrm{i}Ht}\rho_0 \mathrm{e}^{\mathrm{i}Ht}\hat{A}). \tag{1}$$

Due to the recurrence theorem, a finite closed system returns arbitrarily close to its initial state on account of the entirely unitary evolution and never truly equilibrates.[8,9] However, we can focus on the transient non-equilibrium dynamics and define the equilibration in the sense of the time average

$$\rho_{\mathrm{D}} = \lim_{T\to\infty} \frac{1}{T} \int_0^T \mathrm{e}^{-\mathrm{i}Ht}\rho_0 \mathrm{e}^{\mathrm{i}Ht}\,\mathrm{d}t. \tag{2}$$

For the Hamiltonian with non-degenerate energy eigenvalues and non-degenerate energy level differences, ρ_{D} is also called the diagonal ensemble.[10] Thermal equilibrium can be reached as the time average diagonal ensemble is identical with a thermal distribution. In particular, by considering the local observables which are defined only on a small number of sites, the equilibration is easier to achieve according to the Levy's theory.[11–13] One part of an isolated system regards the rest as a bath, thus leading to the non-unitary time evolution, which can be described by an appropriate statistical ensemble depending only on a small number of parameters.

After a global quench, there are three distinct behaviors: (1) For the nonintegrable systems, ergodicity in phase space leads to thermalization finally. (2) For the integrable systems, the conservations of all the constants of motion restrict the microstates only in a small part of the relevant energy shell. So the system relaxes to a nonthermal steady state which can be described by a generalized Gibbs ensemble (GGE).[14–16] The GGE, which was firstly introduced by Jaynes,[15,16] maximizes the entropy under the constraints of the fixed integrals of motion. (3) For the nearly integrable systems, the dynamics of local observables at transient and intermediate-time scales are controlled by the corresponding integrable theory, which is termed prethermalization,[17–19] and finally thermalize in a long time scale.

The thermalization can be explained by the eigenstate thermalization hypothesis (ETH),[20–28] which states that the diagonal matrix elements of the observables are smooth func-

*Project supported by the National Natural Science Foundation of China (Grant No. 11147110) and the Natural Science Youth Foundation of Shanxi, China (Grant No. 2011021003).

†Corresponding author. E-mail: suxq@mail.ustc.edu.cn

© 2020 Chinese Physical Society and IOP Publishing Ltd

tions of the energy, and the off-diagonal elements are exponentially small in the system size. For the local observable $\hat{A}$, the ETH postulates that[22–25]

$$\langle E_m|\hat{A}|E_n\rangle = f_A(\overline{E})\delta_{mn} + \mathrm{e}^{-S(\overline{E})/2}R_{mn}, \tag{3}$$

where $\overline{E} = (E_m + E_n)/2$, $S(E)$ is the thermodynamic entropy at energy E, and $f_A(E)$ are smooth functions of E, while the fluctuations R_{mn} are of order one. To understand the thermalization in isolated quantum systems in view of the ETH, we consider an initial state $|\Psi_0\rangle = \sum_n a_n|n\rangle$, where $|n\rangle$ are the eigenstates of the Hamiltonian H. The time evolution is $|\Psi(t) = \exp[-\mathrm{i}\hat{H}t]|\Psi_0\rangle = \sum_n \exp[-\mathrm{i}E_n t]|n\rangle$. The expectation values of the observable can be written as

$$\begin{aligned} A(t) &= \langle\Psi(t)|\hat{A}|\Psi(t)\rangle \\ &= \sum_n |a_n|^2 A_{nn} + \sum_{m\neq n} a_m^* a_n \,\mathrm{e}^{\mathrm{i}(E_m - E_n)t} A_{mn}. \end{aligned} \tag{4}$$

According to the ETH, the off-diagonal matrix elements of the observables are exponentially small, and the smooth dependence of A_{nn} on the energy makes the eigenstates in the narrow window of a microcanonical ensemble have almost the same expectation values, leading to the thermalization finally.

2. Generalized Gibbs ensemble

The lack of thermalization after the quantum quench for an integrable system can be explained as the conservations of the numerous constants of motion whose values are depend on the initial state. The time-averaged steady state after relaxation reaches a generalized Gibbs ensemble that keeps track of the initial values of all the constants of motion. The density matrix of the GGE can be written as

$$\rho_{GGE} = \frac{1}{Z}\mathrm{e}^{-\sum_n \lambda_n I_n}, \tag{5}$$

where Z is a normalization and I_n are local conserved quantities operators with

$$[I_n, I_m] = [I_n, H] = 0. \tag{6}$$

The Lagrange mutipliers λ_n are fixed by the requirements

$$\langle\Psi_0|I_n|\Psi_0\rangle = \mathrm{Tr}[\rho_{\mathrm{GGE}} I_n]. \tag{7}$$

The GGE is fundamentally different from the thermal ensembles because through the specific values of the Lagrange multipliers, they retain a large amount of information about the initial state.

The GGE has been demonstrated in many quench proposals,[29–33] however there were also some counterexamples in previous reports,[34–36] revealing the inefficacy of the GGE to describe the quantum quench within some integrable systems. Goldstone[34] diagonalized the attractive Lieb–Liniger gas and the XXZ model with the Bethe ansatz equations, and found that there are many eigenstates which correspond to the same conserved quantities but their Bethe densities are different, making the GGE which are uniquely constructed by these conserved quantities unable to catch all the pictures of the post quench systems. Pozsgay[35] also calculated the short ranged spin correlators for the quench in the XXZ spin model, and found that they do not agree with the GGE predictions. In this paper, we will study the applicability of the GGE in the quantum quench of the Dicke model.

3. The Dicke model

The atomic ensembles which couple with an electromagnetic cavity have been widely used in quantum information processing.[37–42] The Dicke model[43–45] describes a collection of N two-level systems, such as two level atoms, interacting with a single Bosonic mode via a dipole interaction with coupling strength λ. The Hamiltonian can be written as

$$H = \sum_{i=1}^{N} \Delta s_i^z + \omega a^\dagger a + \frac{\lambda}{\sqrt{N}}\sum_{i=1}^{N}(a^\dagger + a)(s_i^+ + s_i^-), \tag{8}$$

where s_i describes the dynamics of the two-level systems with energy splitting Δ, and a ($a^\dagger$) stands for the annihilation (creation) operator of the Bosonic field with frequency ω. Here we set $\hbar = 1$. The coupling between the atoms and the field has been rescaled by $1/\sqrt{N}$ in order to avoid energy divergence in the thermodynamic limit. The Dicke model has a quantum phase transition from the normal phase to the superradiant phase at a quantum critical point $\lambda_{\mathrm{c}} = \sqrt{\Delta\omega}/2$. The transition is characterized by the breaking of the parity symmetry, leading to a phase in which the photons in the system ground state is proportional to N.

By introducing the collective atomic operators

$$J_z = \sum_i s_i^z; \quad J_\pm = \sum_i s_i^\pm, \tag{9}$$

which obey the usual angular momentum communication relations

$$[J_z, J_\pm] = \pm J_\pm; \quad [J_+, J_-] = 2J_z, \tag{10}$$

the Hamiltonian can be written as

$$H = \Delta J_z + \omega a^\dagger a + \frac{\lambda}{\sqrt{N}}(a^\dagger + a)(J_+ + J_-). \tag{11}$$

The Hilbert space is spanned by the product of the Dicke states $|j,m\rangle$, which are the eigenstates of J^2 and J_z,

$$J^2|j,m\rangle = j(j+1)|j,m\rangle; \quad J_z|j,m\rangle = m|j,m\rangle, \tag{12}$$

and the Fock states $|n\rangle$ of the field. Here we assume that the resonance condition is satisfied and further set $\Delta = \omega = 1$.

The nonequilibrium dynamics of the Dicke model have been studied by many authors.[46–52] The statistics of the work in the quench process were calculated,[47,48] and used to verify the anomalous thermalization,[48] and the dynamics of the total occupation of the bosonic modes were obtained. Reference [49] focused on the post quench dynamics of the survival probability and the strength function which denotes the local density of states, and discussed the connection with the excited state quantum phase transitions. In this paper, we study the quench dynamics in the Dicke model with the different

quench parameters, calculate the post quench energy level occupations, and compare them with the GGE for the integrable situation in the thermodynamic limit (Section 4). Besides, with the thermal ensembles for the non-integrable finite systems (Section 5), the effect of the equilibrium phase transition is also discussed.

4. Quench in the thermodynamic limit

We firstly consider the quench in the thermodynamic limit with infinite number of atoms. The Hamiltonian is integrable by using the Holstein–Primakoff transformation[53–56]

$$J_+ = b^\dagger\sqrt{2j-b^\dagger b},\ \ J_- = \sqrt{2j-b^\dagger b}\,b,\ \ \ J_z = (b^\dagger b - j), \tag{13}$$

where the Bosonic field operators obey $[b,b^\dagger]=1$.

For the normal phase with $\lambda<\lambda_c$, we can neglect the low population term, and rewrite the Hamiltonian as

$$H = \Delta b^\dagger b + \omega a^\dagger a + \lambda(a^\dagger + a)(b^\dagger + b) - j\Delta. \tag{14}$$

Then by introducing two position and momentum operators for the Bosonic modes

$$\begin{aligned} x &= \frac{1}{\sqrt{2\omega}}(a^\dagger + a), \quad p_x = \mathrm{i}\sqrt{\frac{\omega}{2}}(a^\dagger - a); \\ y &= \frac{1}{\sqrt{2\Delta}}(b^\dagger + b), \quad p_y = \mathrm{i}\sqrt{\frac{\Delta}{2}}(b^\dagger - b); \end{aligned} \tag{15}$$

and rotating the coordinate axis by an angle $\gamma=\pi/4$

$$q_1 = \frac{1}{\sqrt{2}}(x-y), \quad q_2 = \frac{1}{\sqrt{2}}(x+y), \tag{16}$$

the Hamiltonian thus can be written as two uncoupled harmonic oscillators

$$H = \frac{1}{2}(\varepsilon_-^2 q_1^2 + p_1^2 + \varepsilon_+^2 q_2^2 + p_2^2 - \omega - \Delta) - j\Delta, \tag{17}$$

where $\varepsilon_\pm^2 = \frac{1}{2}\left(\Delta^2+\omega^2 \pm \sqrt{(\Delta^2-\omega^2)^2+16\lambda^2\Delta\omega}\right)$.

Two new Bosonic modes can be defined from Eq. (17) as

$$\begin{aligned} c_1 &= \sqrt{\frac{\varepsilon_-}{2}}q_1 + \mathrm{i}\sqrt{\frac{1}{2\varepsilon_-}}p_1, \quad c_1^\dagger = \sqrt{\frac{\varepsilon_-}{2}}q_1 - \mathrm{i}\sqrt{\frac{1}{2\varepsilon_-}}p_1, \\ c_2 &= \sqrt{\frac{\varepsilon_+}{2}}q_2 + \mathrm{i}\sqrt{\frac{1}{2\varepsilon_+}}p_2, \quad c_2^\dagger = \sqrt{\frac{\varepsilon_+}{2}}q_2 - \mathrm{i}\sqrt{\frac{1}{2\varepsilon_+}}p_2. \end{aligned} \tag{18}$$

Therefore the Hamiltonian can be diagonalized as

$$H = \varepsilon_- c_1^\dagger c_1 + \varepsilon_+ c_2^\dagger c_2 + \frac{1}{2}(\varepsilon_- + \varepsilon_+ - \omega - \Delta) - j\Delta. \tag{19}$$

The wave functions of the energy eigenstates can thus be written as two independent harmonic oscillators

$$\begin{aligned} \psi_{m,n}(\lambda<\lambda_c,x,y) = {}& \frac{(1-4\lambda^2)^{\frac{1}{4}}}{\sqrt{\pi 2^{m+n}m!n!}}\exp\left[-\frac{x^2+y^2}{2} - 2\lambda xy\right] \\ & \times H_m\left[\sqrt{\frac{1+2\lambda}{2}}(x+y)\right] H_n\left[\sqrt{\frac{1-2\lambda}{2}}(x-y)\right], \end{aligned} \tag{20}$$

where H_n is the n-order Hermite polynomial, and the ground state is $\psi_{0,0}(\lambda,x,y)$ with no excitation. The parities of the two modes can be written as

$$\Pi_1 = \exp[\mathrm{i}\pi c_1^\dagger c_1], \quad \Pi_2 = \exp[\mathrm{i}\pi c_2^\dagger c_2]. \tag{21}$$

For the superradiant phase with $\lambda>\lambda_c$, in which both the field and the atoms are macroscopic excited, we can not simply neglect the low excitation term like in the normal phase. In order to diagonalize the Holstein–Primakoff Hamiltonian, we firstly displace the two Bosonic modes as[56]

$$a^\dagger \to c^\dagger + \sqrt{\alpha}; \quad b^\dagger \to d^\dagger - \sqrt{\beta}, \tag{22}$$

and then introduced the position–momentum representation

$$\begin{aligned} X &= \frac{1}{\sqrt{2\omega}}(c^\dagger + c), \quad P_X = \mathrm{i}\sqrt{\frac{\omega}{2}}(c^\dagger - c); \\ Y &= \frac{1}{\sqrt{2\tilde{\omega}}}(d^\dagger + d), \quad P_Y = \mathrm{i}\sqrt{\frac{\tilde{\omega}}{2}}(d^\dagger - d); \end{aligned} \tag{23}$$

where $\tilde{\omega} = (\Delta/2\mu)(1+\mu)$ with $\mu = \Delta\omega/4\lambda^2$. Then rotate the XY plane by

$$X = Q_1\cos\gamma' + Q_2\sin\gamma', \ \ Y = -Q_1\sin\gamma' + Q_2\cos\gamma', \tag{24}$$

with the angle γ' obeying

$$\tan(2\gamma') = \frac{2\omega\Delta\mu^2}{\Delta^2 - \mu^2\omega^2}. \tag{25}$$

The Hamiltonian can be diagonalized as

$$\begin{aligned} H' = {}& \varepsilon_-' e_1^\dagger e_1 + \varepsilon_+' e_2^\dagger e_2 - j\left(\frac{2\lambda^2}{\omega} + \frac{\Delta^2\omega}{8\lambda^2}\right) \\ & + \frac{1}{2}\left[\varepsilon_-' + \varepsilon_+' - \frac{\Delta}{2\mu}(1+\mu) - \omega - \frac{2\lambda^2}{\omega}(1-\mu)\right] \end{aligned} \tag{26}$$

with the oscillator energies

$$2\varepsilon_\pm'^2 = \frac{\Delta^2}{\mu^2} + \omega^2 \pm \sqrt{\left(\frac{\Delta^2}{\mu^2} - \omega^2\right)^2 + 4\omega^2\Delta^2}. \tag{27}$$

The wave functions of the energy eigenstates can thus be written as

$$\begin{aligned} \psi_{m,n}(\lambda>\lambda_c,X,Y) = {}& \frac{(\varepsilon_+'\varepsilon_-'\Delta)^{\frac{1}{4}}}{(\tilde{\omega})^{\frac{1}{4}}\sqrt{\pi 2^{m+n}m!n!}} \\ & \times \exp\left[\frac{-\varepsilon_+'[\sin\gamma' X + \sqrt{\frac{\Delta}{\tilde{\omega}}}\cos\gamma' Y]^2}{4}\right] \\ & \times H_m\left[\sqrt{\varepsilon_+'}(\sin\gamma' X + \sqrt{\frac{\Delta}{\tilde{\omega}}}\cos\gamma' Y)\right] \\ & \times \exp\left[\frac{-\varepsilon_-'\left[\cos\gamma' X - \sqrt{\frac{\Delta}{\tilde{\omega}}}\sin\gamma' Y\right]^2}{4}\right] \\ & \times H_m\left[\sqrt{\varepsilon_-'}(\cos\gamma' X - \sqrt{\frac{\Delta}{\tilde{\omega}}}\sin\gamma' Y)\right]. \end{aligned} \tag{28}$$

The excitations destroy the conservations of the parities defined in Eq. (21), and two new conserved parity operators can be constructed by using the new Bosonic modes as

$$\Pi_1' = \exp[\mathrm{i}\pi e_1^\dagger e_1], \quad \Pi_2' = \exp[\mathrm{i}\pi e_2^\dagger e_2]. \tag{29}$$

We assume that the system is prepared initially in the

ground state with λ_0, which then is suddenly changed to λ. Thus the post quench wave functions can be written as

$$|\psi(t)\rangle = \sum_{mn} a_{mn} \mathrm{e}^{-\mathrm{i}E_{mn}t} \psi_{m,n}(\lambda), \tag{30}$$

where the coefficients $a_{mn} = \langle \psi_{m,n}(\lambda) | \psi_{0,0}(\lambda_0) \rangle$, and E_{mn} are the energy eigenvalues of $\psi_{m,n}$. The energy-level occupations of the post quench system $P_{mn} = |a_{mn}|^2$ are schematically plot in the left column of Fig. 1.

It is considered that the post quench systems can be described by the generalized Gibbs ensembles which are constructed on the constants of motion. For the single mode harmonic oscillator, the natural conserved quantities are the total energy and the parity.[57] So we obtain the GGE by employing a set of four independent conserved quantities: the energies and the parities of the two harmonic modes. For comparison, the corresponding canonical ensembles are also obtained as

$$P^T_{mn} = \frac{1}{Z} \exp\left(-\frac{m\varepsilon_+ + n\varepsilon_-}{T}\right), \tag{31}$$

where $Z = \sum_{mn} \exp[-(m\varepsilon_+ + n\varepsilon_-)/T]$ is the partition function, and we set the Boltzman constant $k = 1$ for simplify. It will be convenient to define the effective Gibbs temperature T by employing

$$\sum_{mn} P^T_{mn}(m\varepsilon_+ + n\varepsilon_-) = \sum_{mn} P_{mn}(m\varepsilon_+ + n\varepsilon_-). \tag{32}$$

We comparatively plot the three ensembles for the different n with certain m in the right column of the Fig. 1. The solid, dashed, and dotted lines are the diagonal ensemble, the GGE, and the canonical ensemble, respectively. We can find that the occupations of the canonical ensembles decrease with the increase of quantum number n, but the diagonal ensembles and the GGE present nonmonotonic structures which depend on the initial states for some quench parameters. For the quench complete in the normal phase with $\lambda, \lambda_0 < \lambda_c$, the diagonal ensemble is even directly coincident with the GGE. Therefore, there is no doubt that for any local observables, the same expectations will be obtained for the two ensembles. But for the quench target to a final superradiant phase, there are obvious divergences between the diagonal ensemble and the GGE.

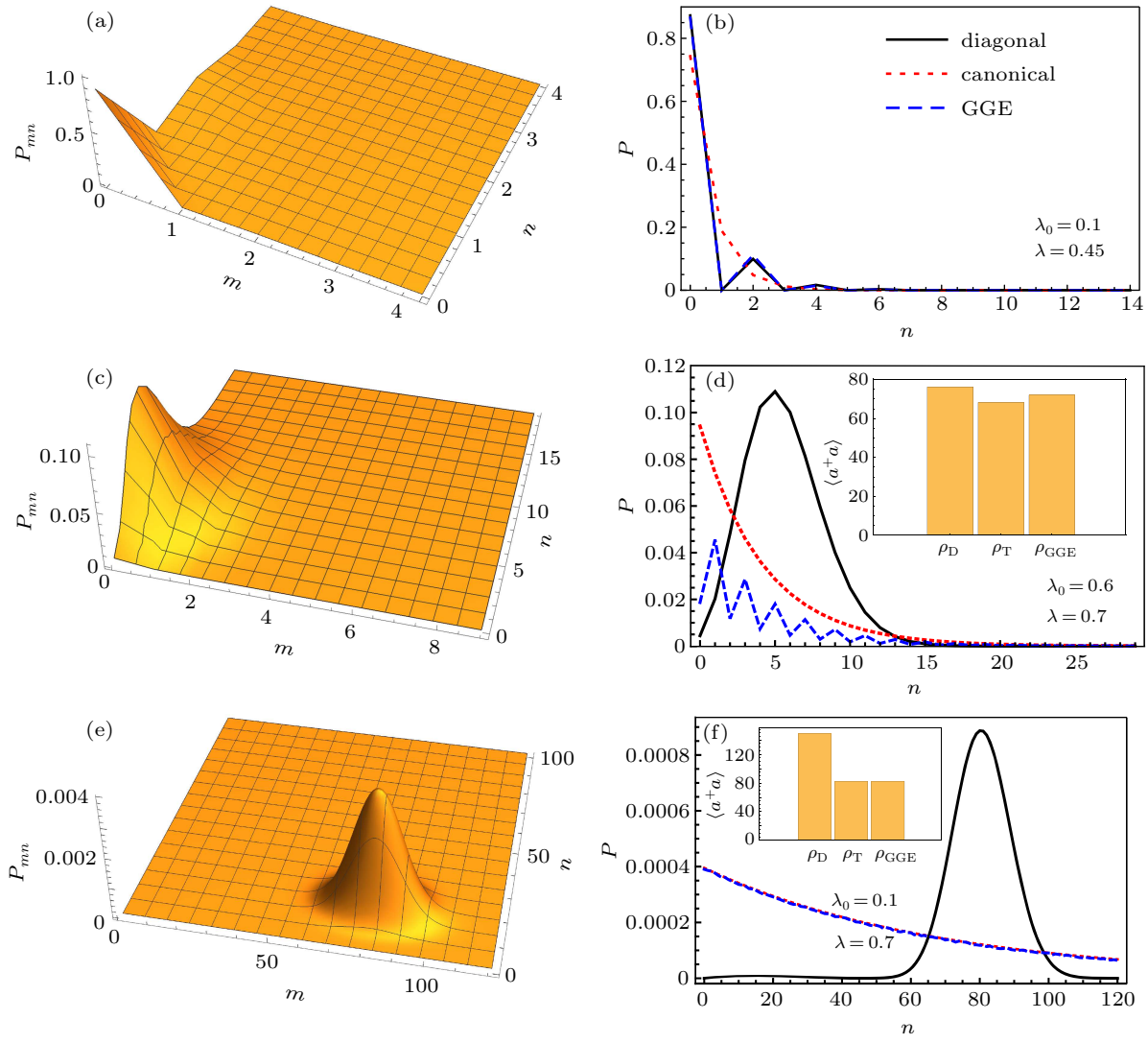


Fig. 1. Quantum quench for the Dicke model in the thermodynamic limit with different quench parameters. The left column shows the post quench energy-level occupations P_{mn}, and the right column shows the contrastive diagrams of the diagonal ensemble (solid), canonical ensemble (dotted), and the GGE (dashed) for different n with certain m.

To further estimate the validity of the GGE, we focus on the local observables defined on the subsystem. We calculate the average values of the numbers of photons $\langle a^{\dagger}a\rangle$ for the three ensembles, as seen in the insets of Figs. 1(d) and 1(f). The divergence between the GGE and the diagonal ensemble can be explained as follows. The GGE introduces the distribution of exponential decay with the increase of the energy levels under the restrictions of a set of conserved quantities. Thus, it is applicable to describe the natural quench in the normal phase which mostly populates in the low energy levels. But in the superradiant phase, the intense excitations lead to the population inversion in the energy levels, as seen in Figs. 1(c) and 1(e), making the GGE fail to describe the energy-level occupations of the post quench system.

It is also worth mentioning that for the quench over the phase transition point from an initial normal phase ground state with $\lambda_0 < \lambda_c$ to the final superradiant phase with $\lambda > \lambda_c$, the GGE and the canonical ensemble have the similar distribution (see Fig. 1(f)). Since the superradiant excitations destroy the symmetry of the parities $\Pi_{1,2}$, the displacements Eq. (22) and the rotations Eq. (24) in the parameters space lead to the identical Lagrange multipliers (see Eq. (5)) for the two new parities with $\langle\Pi_1'\rangle = \langle\Pi_2'\rangle = 0$. The GGE with exponential decay depending only on the energy levels is eventually constructed analogous to the canonical ensemble.

5. Quench in the finite system

The Dicke model is exactly integrable in the thermodynamic limit, but for the finite systems, chaotic characteristics emerge as the result of the non-integrability. These can be described by the energy spectrum statistical theory.[58] For the integrable systems, the numerous conserved quantities lead to the energy level degeneracy (level crossing in the spectrum). The nearest-neighbor level spacing distribution (LSD) $P(S)$ has a maximum at $S \to 0$, with a $P(S)$ given by the Poisson distribution $P(S) = \mathrm{e}^{-S}$. For the non-integrable systems, the level repulsion leads to the Wigner–Dyson distribution $P(S) = \frac{\pi S}{2}\mathrm{e}^{-\pi S^2/4}$. The integrability can be characterized by the quantity η that was defined in Ref. [56] as

$$\eta = \left|\frac{\int_0^{S_0}[P(S) - P_{\mathrm{W}}(S)]dS}{\int_0^{S_0}[P_{\mathrm{P}}(S) - P_{\mathrm{W}}(S)]dS}\right|, \tag{33}$$

where $S_0 = 0.472913\cdots$, $P_{\mathrm{P}}(S)$ and $P_{\mathrm{W}}(S)$ are respectively the Poisson and Wigner–Dyson distributions. Thus, $\eta = 0$ indicates the Wigner–Dyson distribution $P(S) = P_{\mathrm{W}}(S)$, and $\eta = 1$ for the Poisson $P(S) = P_{\mathrm{P}}(S)$. We numerically diagonalize the finite Dicke Hamiltonian and obtain the energy spectra. The LSD can be constructed from a large number of the levels from the spectrum which we initially unfold to remove energy scale variation.[59] We calculate the η for the systems with the number of atoms $N = 200$ and different truncated numbers of photons M, as shown in Fig. 2. With the increase of the truncated numbers of photons, the system tends to be integrable.

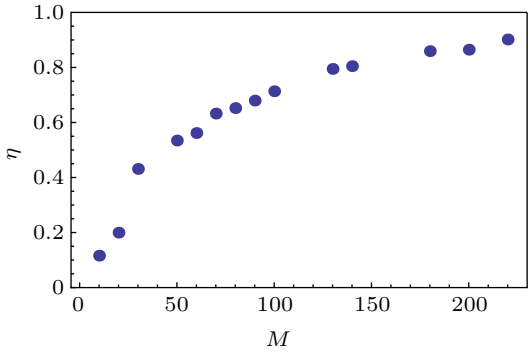


Fig. 2. The integrability η as a function of different truncated numbers of photons M for the systems with the number of atoms $N = 200$ and $\lambda = 0.7$.

We numerically calculate the quench process in the finite Dicke model. Here for comparison, we selecte the similar quench parameters with the infinite situation in Section 4. Thermalization is considered[13,60,61] to take place when the diagonal ensemble gives the same predictions with the microcanonical ensemble for the local operators $\hat{A}$ as

$$\sum_n P_n A_{nn} = \langle\hat{A}\rangle_{\mathrm{mic}}(E_0) = \frac{1}{N_{E_0,\Delta E}}\sum_{|E_0 - E_i| < \Delta E/2} A_{ii}, \tag{34}$$

where E_0 is the mean energy of the post quench system, ΔE is the width of the energy window centered at E_0, and $N_{E_0,\Delta E}$ is the number of the energy eigenstates in the window.

We calculate the reduced density matrix of the subsystem that considers only the atoms, which can be obtained by tracing all the degrees of freedom of the Boson field as

$$\rho_{ij} = \mathrm{Tr}_B\rho. \tag{35}$$

We compare the diagonal elements of the reduced density matrix with the results of the microcanonical ensemble and the canonical ensemble, as seen in the left column of Fig. 3. The LSD $P(S)$ (bar chart) of the corresponding target Hamiltonian are plot in Figs. 3(b) and 3(d), the solid and dashed lines are respectively the contrastive Wigner–Dyson and Poisson distributions.

To estimate the rationality of the microcanonical ensemble, we introduce the Hellinger distance[62] of two distributions P and Q, which is defined as

$$D_{\mathrm{H}} = \frac{1}{\sqrt{2}}\sqrt{\sum_i(\sqrt{P_i} - \sqrt{Q_i})^2}, \tag{36}$$

where $D_{\mathrm{H}} = 0$ indicates that P and Q are the same distributions, and $D_{\mathrm{H}} = 1$ means $P_i = 0$ for each i with $Q_i \neq 0$ and vice versa. We calculate the Hellinger distance of the distributions of the diagonal elements of the reduced density matrix of the post quench system and the microcanonical ensemble for the different numbers of atoms and the certain truncated numbers of photons M, as shown in Fig. 3(f). We can find that, the D_{H} roughly increases with the increase of the numbers of atoms, which is in line with the Levy's theorem. The fluctuation is derived from the fixed width of the energy windows of the microcanonical ensemble.

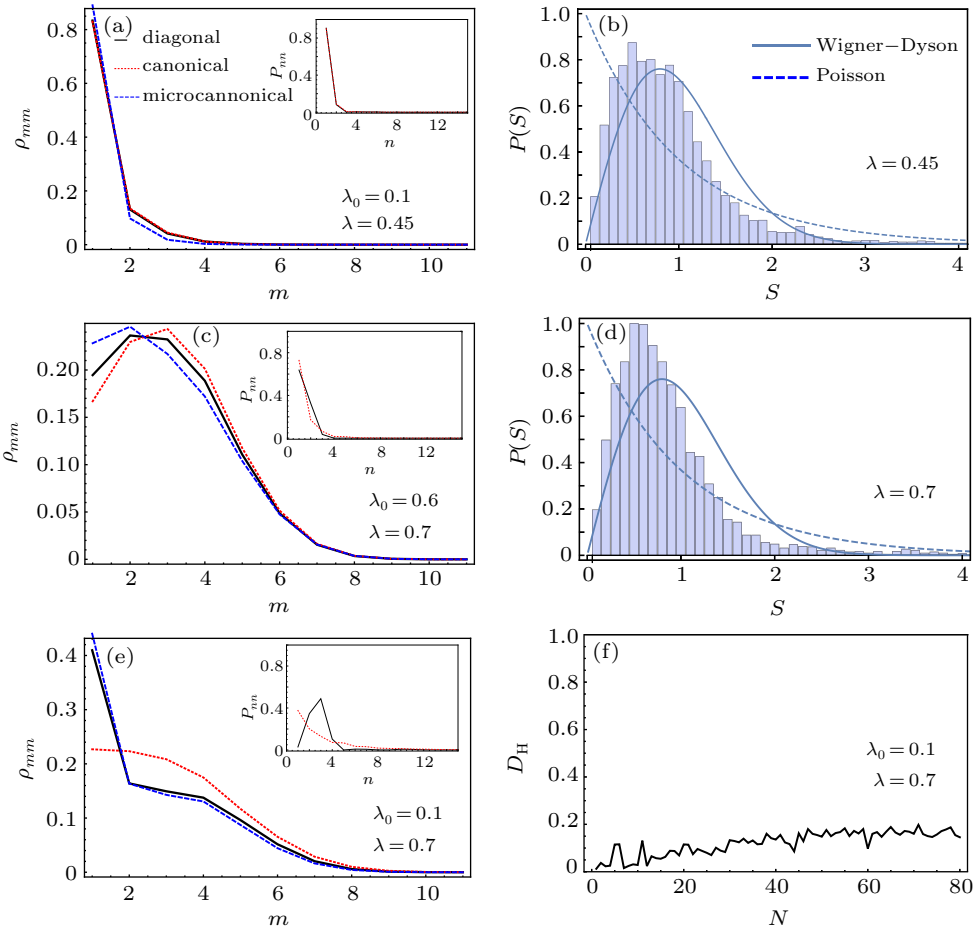


Fig. 3. Quantum quench in the finite Dicke model with the number of atoms $N = 10$ and a truncated number of photons of the Boson field $M = 200$ for the different quench parameters. The left column shows the diagonal elements of the reduced density matrix of the subsystem that considers only the atoms for the different ensembles. The insets are the energy-level occupations of the post quench system (solid lines) and the corresponding canonical ensembles (dotted lines) for the entire system. (b) and (d) The LSD $P(S)$ (bar chart) of the corresponding target Hamiltonian, the solid and dashed lines are respectively the contrastive Wigner–Dyson and Poisson distributions. (f) The Hellinger distance of the distributions of the diagonal elements of the reduced density matrix of the post quench system and the microcanonical ensemble for the different numbers of atoms and the same truncated number of photons $M = 200$, the width of the energy window is fixed set to $\Delta E = 1$.

It is also interesting that for the quench within the normal phase, the energy-level occupations of the post quench system decrease exponentially with the increase of the energy levels. Thus it is straightly identical with the canonical ensemble. But it is not the case for the quench to the superradiant phase. To further study the influence of the equilibrium phase transition on the quench process, we calculate the quench to the different target coupling strengths λ from the same initial normal phase ground state with $\lambda_0 = 0.1$. The effective temperature T and the Hellinger distance between the post quench system and the canonical ensemble as a function of different λ are plot respectively in Figs. 4(a) and 4(b). Abrupt change takes place at the critical point $\lambda_{\rm c}$ both for the distance $D_{\rm H}$ and the derivative of the temperature T. For the quench within the normal phase, low excitation in the post quench system makes the effective temperature close to zero. So it can be holistically described by the canonical ensemble. For the quench to the superradiant phase, thermalization is demonstrated based on the consistence with the microcanonical ensemble.

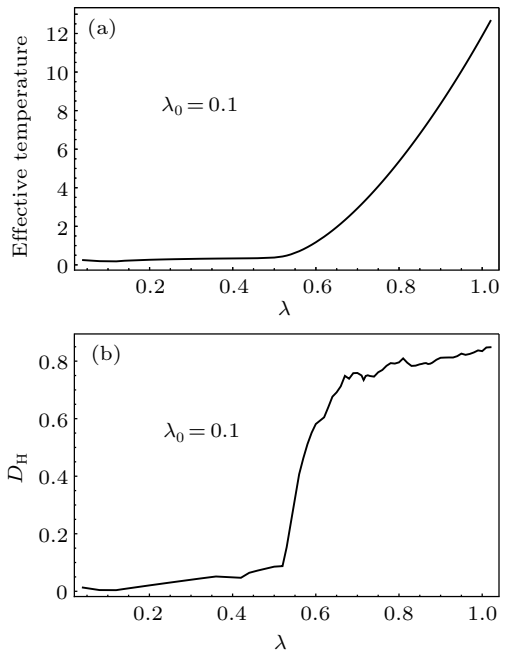


Fig. 4. The effective temperature T (a) and the Hellinger distance $D_{\rm H}$ (b) between the post quench system and the corresponding canonical ensemble as a function of different target coupling strength λ.

6. Conclusion

The generalized Gibbs ensemble is considered to describe the expectations of the local observables in the integrable system after a quantum quench. But our research on the integrable Dicke model shows that the GGE can describe the post quench system effectively only for the quench within the normal phase. The post quench energy-level occupations obviously depend on the pre-quench initial state and the overlap with the eigenstates of the post quench Hamiltonian. The different initial states with the same values of a complete set of conserved quantities are not necessary quenched to the same steady state. The excitations in the superradiant phase lead to the divergence from the usual exponential distribution under the restrictions of the conserved quantities, resulting in the failure of the GGE. Thermalization after the quench in the non-integrable finite system is also studied, and the canonical ensemble is accord with the post quench occupations only within the normal phase. For the quench cross over the phase transition critical point, sudden changes of the Hellinger distance and the derivative of the effective temperature are present. The thermalization is also studied by comparing with the results of the microcanonical ensemble.

References

[1] Kinoshita T, Wenger T and Weiss D S 2006 *Nature* **440** 900
[2] Tang Y, Kao W, Li K Y, Seo S, Mallayya K, Rigol M, Gopalakrishnan S and Lev B L 2018 *Phys. Rev. X* **8** 021030
[3] Greiner M, Mandel O, Hänsch T W and Bloch I 2002 *Nature* **419** 51
[4] Rigol M 2009 *Phys. Rev. A* **80** 053607
[5] Khatami E, Pupillo G, Srednicki M and Rigol M 2013 *Phys. Rev. Lett.* **111** 050403
[6] Sorg S, Vidmar L, Pollet L and Heidrich-Meisner F 2014 *Phys. Rev. A* **90** 033606
[7] Gogolin C, Mueller M P and Eisert J 2011 *Phys. Rev. Lett.* **106** 040401
[8] Bocchieri P and Loinger A 1957 *Phys. Rev.* **107** 337
[9] Percival I C 1961 *J. Math. Phys.* **2** 235
[10] Cassidy A C, Clark C W and Rigol M 2011 *Phys. Rev. Lett.* **106** 140405
[11] Linden N, Popescu S, Short A J and Winter A 2009 *Phys. Rev. E* **79** 061103
[12] Goldstein S, Lebowitz J L, Tumulka R and Zanghì N 2006 *Phys. Rev. Lett.* **96** 050403
[13] Popescu S, Short A J and Winter A 2006 *Nat. Phys.* **2** 754
[14] Rigol M, Dunjko V, Yurovsky V and Olshanii M 2007 *Phys. Rev. Lett.* **98** 050405
[15] Jaynes E T 1957 *Phys. Rev.* **106** 620
[16] Jaynes E T 1957 *Phys. Rev.* **108** 171
[17] Berges J, Borsànyi S and Wetterich C 2004 *Phys. Rev. Lett.* **93** 142002
[18] Marcuzzi M, Marino J, Gambassi A and Silva A 2013 *Phys. Rev. Lett.* **111** 197203
[19] Gring M, Kuhnert M, Langen T, Kitagawa T, Rauer B, Schreitl M, Mazets I, Smith D A, Demler E and Schmiedmayer J 2012 *Science* **337** 1318
[20] Srednicki M 1994 *Phys. Rev. E* **50** 888
[21] Srednicki M 1999 *J. Phys. A: Math. Gen.* **32** 1163
[22] Rigol M, Dunjko V and Olshanii M 2008 *Nature* **452** 854
[23] Rigol M 2009 *Phys. Rev. Lett.* **103** 100403
[24] Rigol M and Santos L F 2010 *Phys. Rev. A* **82** 011604
[25] D'Alessio L, Kafri Y, Polkovnikov A and Rigol M 2016 *Adv. Phys.* **65** 239
[26] Deutsch J M 1991 *Phys. Rev. A* **43** 2046
[27] Biroli G, Kollath C and Läuchli A M 2010 *Phys. Rev. Lett.* **105** 250401
[28] Steinigeweg R, Khodja A, Niemeyer H, Gogolin C and Gemmer J 2014 *Phys. Rev. Lett.* **112** 130403
[29] Langen T, Erne S, Geiger R, Rauer B, Schweigler T, Kuhnert M, Rohringer W, Mazets I E, Gasenzer T and Schmiedmayer J 2015 *Science* **348** 207
[30] Ilievski E, Quinn E and Caux J S 2017 *Phys. Rev. B* **95** 115128
[31] Muralidharan S, Lochan K and Shankaranarayanan S 2018 *Phys. Rev. E* **97** 012142
[32] Vidmar L and Rigol M 2016 *J. Stat. Mech.* 064007
[33] Guryanova Y, Popescu S, Short A J, Silva R and Skrzypczyk P 2016 *Nat. Comm.* **7** 12049
[34] Goldstein G and Andrei N 2014 *Phys. Rev. A* **90** 043625
[35] Pozsgay B, Mestyán M, Werner M A, Kormos M, Zaránd G and Takács G 2014 *Phys. Rev. Lett.* **113** 117203
[36] Mierzejewski M, Prelovšek P and Prosen T 2014 *Phys. Rev. Lett.* **113** 020602
[37] Haroche S, Brune M and Raimond J M 2020 *Nat. Phys.* **16** 243
[38] Zhu H J, Zhang G F, Zhuang L and Liu W M 2018 *Phys. Rev. Lett.* **121** 220403
[39] Fan K M and Zhang G F 2014 *Eur. Phys.J. D* **68** 163
[40] Zhang G F 2007 *Chin. Phys.* **16** 1855
[41] Zhang G F and Liu J 2007 *Chin. Phys.* **16** 3595
[42] Breeze J D, Salvadori E, Sathian J, Alford N M and Kay C W M 2017 *npj Quantum Information* **3** 1
[43] Dicke R H 1954 *Phys. Rev.* **93** 99
[44] Hepp K and Lieb E H 1973 *Ann. Phys. N.Y.* **76** 360
[45] Zhu H J, Xu K, Zhang G F and Liu W M 2020 *Phys. Rev. Lett.* **125** 050402
[46] Kirton P, Roses M M, Keeling J, Dalla T and Emanuele G 2019 *Adv. Quantum Technol.* **2** 1970013
[47] Paraan F N C and Silva A 2009 *Phys. Rev. E* **80** 061130
[48] Relaño A 2018 *Phys. Rev. Lett.* **121** 030602
[49] Kloc M, Stránský P and Cejnar P 2018 *Phys. Rev. A* **98** 013836
[50] Shen L T, Shi Z C, Yang Z B, Wu H Z, Zhong Z R and Zheng S B 2020 *EPJ Quantum Technol.* **7** 1
[51] Ray S, Ghosh A and Sinha S 2016 *Phys. Rev. E* **94** 032103
[52] Chen X M and Wang C 2019 *Chin. Phys. B* **28** 050502
[53] Holstein T and Primakoff H 1949 *Phys. Rev.* **58** 1098
[54] Ressayre E and Tallet A 1975 *Phys. Rev. A* **11** 981
[55] Zhu H J, Zhang G F and Fan H 2016 *Sci. Rep.* **6** 19751
[56] Emary C and Brandes T 2003 *Phys. Rev. E* **67** 066203
[57] Belmonte F and Cuéllar S 2020 arXiv:2001.11621[math-ph]
[58] Haake F 1991 *Quantum Signatures of Chaos* (Berlin: Springer-Verlag)
[59] Guhr T, Müller-Groeling A and Weidenmüller H A 1998 *Phys. Rep.* **299** 189
[60] Reimann P 2008 *Phys. Rev. Lett.* **101** 190403
[61] Riera A, Gogolin C and Eisert J 2012 *Phys. Rev. Lett.* **108** 080402
[62] Rao C R 1995 *Questiió* **19** 23